Journal of Computational and Applied Mathematics 235 (2011) 4272–4282

Contents lists available at ScienceDirect

Journal of Computational and Applied Mathematics

journal homepage: www.elsevier.com/locate/cam

A posteriori error estimates for a finite element approximation of transmission problems with sign changing coefficients

Serge Nicaise *, Juliette Venel

Université de Valenciennes et du Hainaut Cambrésis, LAMAV, FR CNRS 2956, Institut des Sciences et Techniques de Valenciennes, F-59313 - Valenciennes Cedex 9, France

ARTICLE INFO

Article history:
Received 16 September 2010
Received in revised form 21 March 2011

MSC:
65N30
65N15
65N50

Keywords:
A posteriori estimator
Non-positive definite diffusion problems

ABSTRACT

We perform the a posteriori error analysis of residual type of transmission problem with sign changing coefficients. According to Bonnet-BenDhia et al. (2010) [9], if the contrast is large enough, the continuous problem can be transformed into a coercive one. We further show that a similar property holds for the discrete problem for any regular meshes, extending the framework from Bonnet-BenDhia et al. [9]. The reliability and efficiency of the proposed estimator are confirmed by some numerical tests.

1. Introduction

Recent years have witnessed a growing interest in the study of diffusion problems with a sign changing coefficient. These problems appear in several areas of physics, for example in electromagnetism [1–5]. Thus some mathematical investigations have been performed and concern existence results [6,5] and numerical approximations by the finite element methods [5,7–9], with some a priori error analyses. But for such problems the regularity of the solution may be poor and/or unknown and consequently an a posteriori error analysis would be more appropriate. This analysis is the aim of the present paper.

For continuous Galerkin finite element methods, there now exists a large amount of literature on a posteriori error estimations for (positive definite) problems in mechanics or electromagnetism. Usually locally defined a posteriori error estimators are designed. We refer the reader to the monographs [10–13] for a good overview on this topic.

In contrast to that of the recent paper [9], our approach will not use quasi-uniform meshes that are not realistic for an a posteriori error analysis. That is why we improve their finite element analysis in order to allow only regular meshes in Ciarlet's sense [14].

The paper is structured as follows. We recall in Section 2 the "diffusion" problem and the technique from [9] that allows us to establish its well-posedness for sufficiently large contrast; we even present an alternative approach that consists in replacing an ad hoc lifting operator with an extension operator acting from $H^1_+(\Omega_+)$ into $H^1_-(\Omega_-)$ (making the trace on the interface unchanged; see below for the exact notation). In Section 3, we prove that the discrete approximation is well-posed provided the contrast is large enough by introducing an ad hoc discrete version of the above extension operator. The a posteriori error analysis is performed in Section 4, where upper and lower bounds are obtained. Finally in Section 5 some numerical tests are presented that confirm the reliability and efficiency of our estimator.

Let us finish this introduction with some notation used in the remainder of the paper. On D, the $L^2(D)$-norm will be denoted by $\|\cdot\|_D$. The usual norm and seminorm of $H^s(D)$ $(s \geq 0)$ are denoted by $\|\cdot\|_{s,D}$ and $|\cdot|_{s,D}$, respectively. In the

* Corresponding author.
E-mail addresses: Serge.Nicaise@univ-valenciennes.fr (S. Nicaise), Juliette.Venel@univ-valenciennes.fr (J. Venel).

0377-0427/$ – see front matter
doi:10.1016/j.cam.2011.03.028

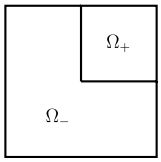

Fig. 1. The domain Ω.

case $D = \Omega$, the index Ω will be omitted. Finally, the notation $a \lesssim b$ means the existence of a positive constant C, which is independent of the mesh size and of the quantities a and b considered, such that $a \leq Cb$. In other words, the constant may depend on the aspect ratio of the mesh and the diffusion coefficient (see below).

2. The boundary value problem

Let Ω be a bounded open domain of $\mathbb{R}^2$ with boundary Γ. We suppose that Ω is split up into two subdomains Ω_+ and Ω_- with a Lipschitz boundary that we suppose to be polygonal, in such a way that

$$\bar{\Omega} = \bar{\Omega}_+ \cup \bar{\Omega}_-, \qquad \Omega_+ \cap \Omega_- = \emptyset;$$

see Fig. 1 for an example.

We now assume that the diffusion coefficient a belongs to $L^\infty(\Omega)$ and is positive (resp. negative) on Ω_+ (resp. Ω_-). Namely there exists $\epsilon_0 > 0$ such that

$$a(x) \geq \epsilon_0, \quad \text{for a. e. } x \in \Omega_+, \tag{1}$$

$$a(x) \leq -\epsilon_0, \quad \text{for a. e. } ; x \in \Omega_-. \tag{2}$$

In this situation we consider the following second-order boundary value problem with Dirichlet boundary conditions:

$$\begin{cases} -\mathrm{div}(a\,\nabla u) = f & \text{in } \Omega, \\ u = 0 & \text{on } \Gamma. \end{cases} \tag{3}$$

The variational formulation of (3) involves the bilinear form

$$B(u, v) = \int_\Omega a \nabla u \cdot \nabla v$$

and the Hilbert space

$$H_0^1(\Omega) = \{u \in H^1(\Omega) : u = 0 \quad \text{on } \Gamma\}.$$

Due to the lack of coercivity of B on $H_0^1(\Omega)$ (see [6,8,9]), this problem does not fit into a standard framework. In [8,9], the proposed approach is to use a bijective and continuous linear mapping $\mathbb{T}$ from $H_0^1(\Omega)$ into itself that allows us to come back to the coercive framework. Namely these authors assume that $B(u, \mathbb{T}v)$ is coercive in the sense that there exists $\alpha > 0$ such that

$$B(u, \mathbb{T}u) \geq \alpha \|u\|_{1,\Omega}^2 \quad \forall u \in H_0^1(\Omega). \tag{4}$$

Hence given $f \in L^2(\Omega)$, by the Lax–Milgram theorem the problem

$$B(u, \mathbb{T}v) = \int_\Omega f \mathbb{T}v \quad \forall v \in H_0^1(\Omega), \tag{5}$$

has a unique solution $u \in H_0^1(\Omega)$. Since $\mathbb{T}$ is an isomorphism, the original problem

$$B(u, v) = \int_\Omega f v \quad \forall v \in H_0^1(\Omega), \tag{6}$$

also has a unique solution $u \in H_0^1(\Omega)$.

In [9], the mapping $\mathbb{T}$ is built by using a trace lifting operator $\mathcal{R}_L$ from $H_{00}^{1/2}(\Sigma)$ into $H_-^1(\Omega_-)$, where $\Sigma = \partial\Omega_- \cap \partial\Omega_+$ is the interface between Ω_- and Ω_+,

$$H_\pm^1(\Omega_\pm) = \{u \in H^1(\Omega_\pm) : u = 0 \text{ on } \partial\Omega_\pm \setminus \Sigma\},$$

and

$$H_{00}^{1/2}(\Sigma) = \{u_{|\Sigma} : u \in H_-^1(\Omega_-)\} = \{u_{|\Sigma} : u \in H_+^1(\Omega_+)\}$$

is the space of the restrictions to Σ of functions in $H^1_-(\Omega_-)$ (or in $H^1_+(\Omega_+)$). This last space may be equipped with the norms

$$\|p\|_{1/2,\pm} = \inf_{\substack{u\in H^1_\pm(\Omega_\pm)\\ p=u_{|\Sigma}}} |u|_{1,\Omega_\pm}.$$

Let us emphasize the fact that by definition of a trace lifting operator, the trace of $\mathcal{R}_L w$ on Σ is w itself.

With the help of such a lifting, a possible mapping $\mathbb{T}_L$ is given by (see [9])

$$\mathbb{T}_L v = \begin{cases} v_+ & \text{in } \Omega_+,\\ -v_- + 2\mathcal{R}_L(v_{+|\Sigma}) & \text{in } \Omega_-, \end{cases}$$

where $v_\pm$ denotes the restriction of v to $\Omega_\pm$. With this choice, it is shown in Proposition 3.1 of [9] that (4) holds if

$$K_{\mathcal{R}_L} = \sup_{\substack{v\in H^1_+(\Omega_+)\\ v\neq 0}} \frac{|B_-(\mathcal{R}_L(v_{|\Sigma}), \mathcal{R}_L(v_{|\Sigma}))|}{B_+(v,v)} < 1, \tag{7}$$

where $B_\pm(u,v) = \int_{\Omega_\pm} a\nabla u\cdot\nabla v$.

For concrete applications, one can make the following particular choice for $\mathcal{R}_L$, that we denote by $\mathcal{R}_p$: for any $\varphi \in H^{1/2}_{00}(\Sigma)$ we define $\mathcal{R}_p(\varphi) = w$ as the unique solution $w \in H^1_-(\Omega_-)$ of

$$\Delta w = 0 \quad \text{in } \Omega_-, \qquad w = \varphi \quad \text{on } \Sigma.$$

With this choice, one obtains that $K_{\mathcal{R}_p} < 1$ if the contrast

$$\frac{\min_{\Omega_+} a}{\max_{\Omega_-} |a|}$$

is large enough; we refer the reader to Section 3 of [9] for more details.

An alternative construction is to use a continuous linear mapping $\mathcal{R}$ from $H^1_+(\Omega_+)$ into $H^1_-(\Omega_-)$ such that

$$(\mathcal{R}v)_{|\Sigma} = v_{|\Sigma} \quad \forall v \in H^1_+(\Omega_+). \tag{8}$$

With the help of such a mapping, we define $\mathbb{T}$ as before by

$$\mathbb{T}v = \begin{cases} v_+ & \text{in } \Omega_+,\\ -v_- + 2\mathcal{R}v_+ & \text{in } \Omega_-, \end{cases}$$

where we recall that $v_\pm$ denotes the restriction of v to $\Omega_\pm$.

Using the same arguments as in the proof of Proposition 3.1 of [9] one can show that (4) holds if

$$K_{\mathcal{R}} = \sup_{\substack{v\in H^1_+(\Omega_+)\\ v\neq 0}} \frac{|B_-(\mathcal{R}v, \mathcal{R}v)|}{B_+(v,v)} < 1. \tag{9}$$

In particular, this condition holds if the contrast satisfies

$$\|\mathcal{R}\|^2 < \frac{\min_{\Omega_+} a}{\max_{\Omega_-} |a|} \tag{10}$$

where $\|\mathcal{R}\|$ means its norm as an operator from $H^1_+(\Omega_+)$ into $H^1_-(\Omega_-)$ equipped with the H^1-seminorm.

Note that the first approach is a subcase of the second one. Both choices can be made according to the circumstances and to the possibility of explicitly calculating (or estimating) the constant $K_{\mathcal{R}_L}$ or $K_{\mathcal{R}}$, but the first case will always yield worse results. Indeed on one hand if $\mathcal{R}_L$ is given then we can define $\mathcal{R}$ by

$$\mathcal{R}v = \mathcal{R}_L(v_{|\Sigma}) \quad \forall v \in H^1_+(\Omega_+),$$

and in that case we have

$$K_{\mathcal{R}} = K_{\mathcal{R}_L}.$$

On the other hand if $\mathcal{R}$ is given then we can take

$$\mathcal{R}_L w = \mathcal{R}(Ew) \quad \forall w \in H^{1/2}_{00}(\Sigma),$$

where E is a trace lifting operator from $H^{1/2}_{00}(\Sigma)$ into $H^1_+(\Omega_+)$ and in this case

$$K_{\mathcal{R}_L} \le K_{\mathcal{R}}.$$

Consequently, in any case, we always have

$$\sup_{\mathcal{R}_L} K_{\mathcal{R}_L} \le \sup_{\mathcal{R}} K_{\mathcal{R}}.$$

We further refer the reader to Section 5 for the use of the second approach.

3. The discrete approximated problem

Here we consider the following standard Galerkin approximation of our continuous problem. We consider a triangulation $\mathcal{T}$ of Ω, that is a "partition" of Ω made of triangles T (closed subsets of $\bar{\Omega}$) whose edges are denoted by e. We assume that this triangulation is regular, i.e., for any element T, the ratio h_T/ρ_T is bounded by a constant $\sigma > 0$ independent of T and of the mesh size $h = \max_{T\in\mathcal{T}} h_T$, where h_T is the diameter of T and ρ_T the diameter of its largest inscribed ball. We further assume that $\mathcal{T}$ is conforming with the partition of Ω, i.e., each triangle is assumed to be either included into $\bar{\Omega}_+$ or into $\bar{\Omega}_-$. With each edge e of the triangulation, we denote by h_e its length and by n_e a unit normal vector (whose orientation can be arbitrary chosen) and define the so-called patch $\omega_e = \cup_{e\subset T} T$, the union of triangles having e as edge. We similarly associate with each vertex x a patch $\omega_x = \cup_{x\in T} T$. For a triangle T, n_T stands for the outer unit normal vector of T. $\mathcal{E}$ (resp. $\mathcal{N}$) represents the set of edges (resp. vertices) of the triangulation. In the sequel, we need to distinguish between edges (or vertices) included in Ω or in Γ; in other words, we set

$$\mathcal{E}_{\rm int} = \{e \in \mathcal{E} : e \subset \Omega\},$$
$$\mathcal{E}_\Gamma = \{e \in \mathcal{E} : e \subset \Gamma\},$$
$$\mathcal{N}_{\rm int} = \{x \in \mathcal{N} : x \in \Omega\}.$$

Problem (6) is approximated by the continuous finite element space:

$$V_h = \left\{v_h \in H_0^1(\Omega) : v_{h|T} \in \mathbb{P}_\ell(T),\ \forall T \in \mathcal{T}\right\}, \tag{11}$$

where ℓ is a fixed positive integer and the space $\mathbb{P}_\ell(T)$ consists of polynomials of degree at most ℓ.

The Galerkin approximation of problem (6) reads now: Find $u_h \in V_h$ such that

$$B(u_h, v_h) = \int_\Omega f v_h \quad \forall v_h \in V_h. \tag{12}$$

Since the bilinear form is not coercive on V_h, as in [9] we need to use a discrete mapping $\mathbb{T}_h$ from V_h into itself defined by

$$\mathbb{T}_h v_h = \begin{cases} v_{h+} & \text{in } \Omega_+, \\ -v_{h-} + 2\mathcal{R}_h(v_{h+}) & \text{in } \Omega_-, \end{cases}$$

where $\mathcal{R}_h$ is a discrete version of the operator $\mathcal{R}$. Here, in contrast to [9] and in order to avoid the use of quasi-uniform meshes (meaningless in an a posteriori error analysis), we take

$$\mathcal{R}_h = I_h\mathcal{R}, \tag{13}$$

where I_h is a sort of Clément interpolation operator [15] and $\mathcal{R}$ is any linear continuous operator from $H^1_+(\Omega_+)$ into $H^1_-(\Omega_-)$ satisfying (8) (see the previous section). More precisely if $\ell = 1$, for $\varphi_h \in V_{h+} = \{v_{h|\Omega_+} : v_h \in V_h\}$, we set

$$I_h\mathcal{R}(\varphi_h) = \sum_{x\in\mathcal{N}_-} \alpha_x\lambda_x,$$

where $\mathcal{N}_- = \mathcal{N}_{\rm int} \cap \bar{\Omega}_-$, λ_x is the standard hat function (defined by $\lambda_x \in V_h$ and satisfying $\lambda_x(y) = \delta_{xy}$) and the $\alpha_x \in \mathbb{R}$ are defined by

$$\alpha_x = \begin{cases} |\omega_x|^{-1} \displaystyle\int_{\omega_x} \mathcal{R}(\varphi_h) & \text{if } x \in \mathcal{N}_{\rm int} \cap \Omega_-, \\ \varphi_h(x) & \text{if } x \in \mathcal{N}_{\rm int} \cap \Sigma, \end{cases}$$

where we recall that ω_x is the patch associated with x, which is simply the support of λ_x. Note that I_h coincides with the Clément interpolation operator $I_{\rm Cl}$ for the nodes in Ω_- and only differs on the nodes on Σ. Indeed let us recall the definition of $I_{\rm Cl}\mathcal{R}(\varphi_h)$ (defined in a Scott–Zhang manner [16] for the points belonging to Σ):

$$I_{\rm Cl}\mathcal{R}(\varphi_h) = \sum_{x\in\mathcal{N}_-} \beta_x\lambda_x$$

with

$$\beta_x = \begin{cases} |\omega_x|^{-1} \displaystyle\int_{\omega_x} \mathcal{R}(\varphi_h) & \text{if } x \in \mathcal{N}_{\rm int} \cap \Omega_-, \\ |e_x|^{-1} \displaystyle\int_{e_x} \mathcal{R}(\varphi_h)\mathrm{d}\sigma & \text{if } x \in \mathcal{N}_{\rm int} \cap \Sigma \text{ with } e_x = \omega_x \cap \Sigma. \end{cases}$$

The definition of I_h aims at ensuring that

$$I_h\mathcal{R}(\varphi_h) = \varphi_h \quad \text{on } \Sigma.$$

For $\ell \geq 2$, we define similarly $I_h\mathcal{R}$ and $I_{\rm Cl}\mathcal{R}$ by using the Lagrange nodal basis (for the Clément interpolation operator based on a polynomial of degree ℓ, see [16]).

Let us now prove that $\mathcal{R}_h$ is uniformly bounded.

Theorem 3.1. *For all $h > 0$ and $\varphi_h \in V_{h+}$, one has*

$$|\mathcal{R}_h(\varphi_h)|_{1,\Omega_-} \lesssim |\varphi_h|_{1,\Omega_+}.$$

Proof. For the sake of simplicity we give the proof for the case $\ell = 1$, the general case is treated in the same manner. Since $\mathcal{R}$ is bounded from $H^1_+(\Omega_+)$ into $H^1_-(\Omega_-)$, one has

$$|\mathcal{R}(\varphi_h)|_{1,\Omega_-} \lesssim |\varphi_h|_{1,\Omega_+}. \tag{14}$$

Hence it suffices to show that

$$|(I - I_h)\mathcal{R}(\varphi_h)|_{1,\Omega_-} \lesssim |\varphi_h|_{1,\Omega_+}. \tag{15}$$

For that purpose, we distinguish the triangles T that have no nodes in $\mathcal{N}_{\text{int}} \cap \Sigma$ from the other ones:

1. If T has no nodes in $\mathcal{N}_{\text{int}} \cap \Sigma$, then $I_h\mathcal{R}(\varphi_h)$ coincides with $I_{\text{Cl}}\mathcal{R}(\varphi_h)$ on T and therefore by a standard property of the Clément interpolation operator, we have
$$|(I - I_h)\mathcal{R}(\varphi_h)|_{1,T} = |(I - I_{\text{Cl}})\mathcal{R}(\varphi_h)|_{1,T} \lesssim \|\mathcal{R}(\varphi_h)\|_{1,\omega_T}, \tag{16}$$
where the patch ω_T is given by $\omega_T = \bigcup_{T' \cap T \neq \emptyset} T'$.
2. If T has at least one node in $\mathcal{N}_{\text{int}} \cap \Sigma$, by the triangle inequality we may write
$$|(I - I_h)\mathcal{R}(\varphi_h)|_{1,T} \leq |(I - I_{\text{Cl}})\mathcal{R}(\varphi_h)|_{1,T} + |(I_{\text{Cl}} - I_h)\mathcal{R}(\varphi_h)|_{1,T}.$$

For the first term of this right-hand side we can still use Clément type arguments and obtain

$$|(I - I_{\text{Cl}})\mathcal{R}(\varphi_h)|_{1,T} \lesssim \|\mathcal{R}(\varphi_h)\|_{1,\omega_T \cap \Omega_-}.$$

It then remains to estimate the second term. For that purpose, we notice that

$$(I_{\text{Cl}} - I_h)\mathcal{R}(\varphi_h) = \sum_{x \in T \cap \Sigma} (\alpha_x - \beta_x)\lambda_x \quad \text{on } T.$$

Hence

$$|(I_{\text{Cl}} - I_h)\mathcal{R}(\varphi_h)|_{1,T} \lesssim \sum_{x \in T \cap \Sigma} |\alpha_x - \beta_x|.$$

Since $\mathcal{R}(\varphi_h) = \varphi_h$ on Σ and due to the definition of I_{Cl}, it follows that for $x \in T \cap \Sigma$,

$$|\alpha_x - \beta_x| = \left| \varphi_h(x) - |e_x|^{-1} \int_{e_x} \varphi_h \mathrm{d}\sigma \right|.$$

Since all norms are equivalent in finite dimensional spaces, we have for all $v_h \in \mathbb{P}_1(e_x)$,

$$|v_h(x)| \lesssim |e_x|^{-1/2} \|v_h\|_{e_x}. \tag{17}$$

Moreover,

$$|e_x|^{-1/2} \left\| \varphi_h - |e_x|^{-1} \int_{e_x} \varphi_h \mathrm{d}\sigma \right\|_{e_x} \lesssim |\varphi_h|_{1/2,e_x}, \tag{18}$$

where here $|\cdot|_{1/2,e_x}$ means the standard $H^{1/2}(e_x)$-seminorm. Thus Inequality (17) with $v_h = \varphi_h - |e_x|^{-1} \int_{e_x} \varphi_h \mathrm{d}\sigma$ and (18) imply that

$$|\alpha_x - \beta_x| \lesssim |\varphi_h|_{1/2,e_x}.$$

Altogether we have shown that

$$|(I - I_h)\mathcal{R}(\varphi_h)|_{1,T} \lesssim \|\mathcal{R}(\varphi_h)\|_{1,\omega_T \cap \Omega_-} + |\varphi_h|_{1/2,\omega_T \cap \Sigma}. \tag{19}$$

Taking the sum of the square of (16) and of (19), we obtain that

$$|(I - I_h)\mathcal{R}(\varphi_h)|^2_{1,\Omega_-} \lesssim \|\mathcal{R}(\varphi_h)\|^2_{1,\Omega_-} + |\varphi_h|^2_{1/2,\Sigma}.$$

We conclude thanks to (14) and by using a trace estimate that

$$|\varphi_h|_{1/2,\Sigma} \lesssim |\varphi_h|_{1,\Omega+}. \quad \square$$

This theorem and the arguments of Proposition 4.2 of [9] allow us to conclude that (12) has a unique solution provided that the contrast is large enough. Indeed as in the continuous setting we can introduce the discrete mapping $\mathbb{T}_h$ given by

$$\mathbb{T}_h v_h = \begin{cases} v_{h+} & \text{in } \Omega_+, \\ -v_{h-} + 2\mathcal{R}_h(v_{h+}) & \text{in } \Omega_-. \end{cases}$$

Hence we obtain that (see the proof of Proposition 3.1 of [9])

$$B(v_h, \mathbb{T}_h v_h) \geq \gamma_h |v_h|^2_{1,\Omega}$$

for some $\gamma_h > 0$ (that could depend on h) if

$$K_{\mathcal{R}_h} = \max_{\substack{v_h \in V_{h+} \\ v_h \neq 0}} \frac{|B_-(\mathcal{R}_h v_h, \mathcal{R}_h v_h)|}{B_+(v_h, v_h)} < 1. \tag{20}$$

Since $\mathcal{R}_h$ is uniformly bounded in h, setting

$$\alpha = \sup_{h>0} \|\mathcal{R}_h\|_h,$$

where $\|\cdot\|_h$ means the norm as an operator from V_{h+} into V_{h-} equipped with the H^1-seminorm, we get

$$K_{\mathcal{R}_h} \leq \alpha^2 \frac{\max\limits_{\Omega_-} |a|}{\min\limits_{\Omega_+} a}.$$

Therefore the condition (20) holds if

$$\alpha^2 \frac{\max\limits_{\Omega_-} |a|}{\min\limits_{\Omega_+} a} < 1.$$

Hence if the contrast is large enough, namely if

$$\alpha^2 < \frac{\min\limits_{\Omega_+} a}{\max\limits_{\Omega_-} |a|}, \tag{21}$$

we will even get the uniform coercivity of $B(v_h, \mathbb{T}_h v_h)$ (since the upper bound of $K_{\mathcal{R}_h}$ is independent of h).

From the above considerations, we see that we get the well-posedness of the discrete problem if the contrast satisfies (21), which is more restrictive than its continuous counterpart (10). Obviously we cannot give an optimal value of α in its full generality because it is related to the shape regularity of the mesh (see Theorem 3.1). Furthermore from the explanations given at the end of Section 2, the use of $\mathcal{R}_h$ is better than the use of the operator $\mathcal{R}_{L,h} := I_h \mathcal{R}_L$. On the other hand, if we can build an explicit linear mapping $\mathcal{R}_{e,h}$ from V_{h+} to V_{h-} such that

$$(\mathcal{R}_{e,h} v_h)_{|\Sigma} = v_{h|\Sigma} \quad \forall v_h \in V_{h+},$$

and for which we can calculate its norm, then we could expect to obtain a better condition on the contrast. This approach is applied in Section 5 for some particular meshes.

Note that the advantage of our construction of $\mathcal{R}_h$ is that we no longer need the quasi-uniform property of the meshes imposed in [9].

4. The a posteriori error analysis

Error estimators can be constructed in many different ways, for example using residual type error estimators which measure locally the jump of the discrete flux [13]. A different method, based on equilibrated fluxes, consists in solving local Neumann boundary value problems [10] or in using the Raviart–Thomas interpolant [17–20]. Here since the coercivity constant is not explicitly known, we chose the simplest approach of residual type.

The residual estimators are denoted by

$$\eta_R^2 = \sum_{T \in \mathcal{T}} \eta_{R,T}^2, \qquad \eta_J^2 = \sum_{T \in \mathcal{T}} \eta_{J,T}^2, \tag{22}$$

where the indicators $\eta_{R,T}$ and $\eta_{J,T}$ are defined by

$$\eta_{R,T} = h_T \|f_T + \operatorname{div}(a \nabla u_h)\|_T,$$

$$\eta_{J,T} = \sum_{e \in \mathcal{E}_{\text{int}} : e \subset T} h_e^{1/2} \|[\![a \nabla u_h \cdot n_e]\!]\|_e,$$

when f_T is an approximation of f, for instance

$$f_T = |T|^{-1} \int_T f.$$

Note that $\eta_{R,T}^2$ is meaningful if $a_{|T} \in H^1(T)$, for all $T \in \mathcal{T}$.

4.1. The upper bound

Theorem 4.1. *Assume that $a \in L^\infty(\Omega)$ satisfies (1)–(2) and that $a_{|T} \in H^1(T)$, for all $T \in \mathcal{T}$. Assume further that (9) holds. Let $u \in H_0^1(\Omega)$ be the unique solution of Problem (6) and let u_h be its Galerkin approximation, i.e. $u_h \in V_h$, a solution of (12). Then one has*

$$\|\nabla(u - u_h)\| \lesssim \eta_R + \eta_J + \mathrm{osc}(f), \tag{23}$$

where

$$\mathrm{osc}(f) = \left(\sum_{T\in\mathcal{T}} h_T^2 \|f - f_T\|^2\right)^{\frac{1}{2}}.$$

Proof. By the coerciveness assumption (4), we may write

$$\|\nabla(u - u_h)\|^2 \lesssim B(u - u_h, \mathbb{T}(u - u_h)). \tag{24}$$

But we notice that the Galerkin relation

$$B(u - u_h, v_h) = 0 \quad \forall v_h \in V_h$$

holds. Hence by taking $v_h = I_{Cl}\mathbb{T}(u - u_h)$, (24) may be written as

$$\|\nabla(u - u_h)\|^2 \lesssim B(u - u_h, (I - I_{Cl})\mathbb{T}(u - u_h)). \tag{25}$$

Now we apply standard arguments; see for instance [13]. Namely applying elementwise Green's formula and writing for brevity $w = (I - I_{Cl})\mathbb{T}(u - u_h)$, we get

$$\|\nabla(u - u_h)\|^2 \lesssim -\sum_{T\in\mathcal{T}} \int_T \mathrm{div}(a\nabla(u - u_h))w + \sum_{e\in\mathcal{E}_{\mathrm{int}}} \int_e [\![a\nabla(u - u_h)\cdot n]\!] w \,\mathrm{d}\sigma,$$

recalling that $w = 0$ on Γ. By the Cauchy–Schwarz inequality we directly obtain

$$\|\nabla(u - u_h)\|^2 \lesssim \sum_{T\in\mathcal{T}} \|f + \mathrm{div}(a\nabla u_h)\|_T \|w\|_T + \sum_{e\in\mathcal{E}_{\mathrm{int}}} \|[\![a\nabla u_h \cdot n]\!]\|_e \|w\|_e.$$

By standard interpolation error estimates, we get

$$\|\nabla(u - u_h)\|^2 \lesssim \left(\sum_{T\in\mathcal{T}} h_T^2 \|f + \mathrm{div}(a\nabla u_h)\|_T^2 + \sum_{e\in\mathcal{E}_{\mathrm{int}}} h_e \|[\![a\nabla u_h \cdot n]\!]\|_e^2\right)^{1/2} |\mathbb{T}(u - u_h)|_{1,\Omega}.$$

Since $\mathbb{T}$ is an isomorphism, we conclude that

$$\|\nabla(u - u_h)\| \lesssim \left(\sum_{T\in\mathcal{T}} h_T^2 \|f + \mathrm{div}(a\nabla u_h)\|_T^2 + \sum_{e\in\mathcal{E}_{\mathrm{int}}} h_e \|[\![a\nabla u_h \cdot n]\!]\|_e^2\right)^{1/2}.$$

This leads to the conclusion due to the triangle inequality. □

4.2. The lower bound

The lower bound is fully standard since by a careful reading of the proof of Proposition 1.5 of [13], we see that it does not use the positiveness of the diffusion coefficient a. Hence we can state:

Theorem 4.2. *Let the assumptions of Theorem 4.1 be satisfied. Assume furthermore that $a_{|T}$ is constant for all $T \in \mathcal{T}$. Then for each element $T \in \mathcal{T}$ the following estimate holds:*

$$\eta_{R,T} + \eta_{J,T} \leq |u - u_h|_{1,\omega_T} + \mathrm{osc}(f, \omega_T),$$

where

$$\mathrm{osc}(f, \omega_T)^2 = \sum_{T'\subset\omega_T} h_{T'}^2 \|f - f_{T'}\|_{T'}^2.$$

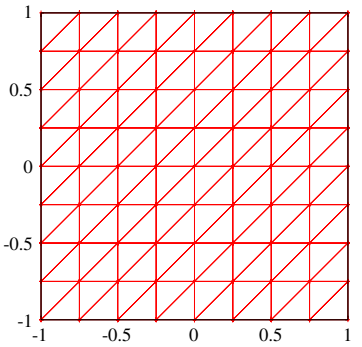

Fig. 2. A uniform mesh for $h = 0.25$.

5. Numerical results

5.1. The polynomial solution

In order to illustrate our theoretical predictions, this first numerical test consists in validating our computations on a simple case, using a uniform refinement process. Let Ω be the square $(-1, 1)^2$, $\Omega_+ = (0, 1) \times (-1, 1)$ and $\Omega_- = (-1, 0) \times (-1, 1)$. We assume that $a = 1$ on Ω_+ and $a = \mu < 0$ on Ω_-. In such a situation we can take

$$\mathcal{R}(v_+)(x, y) = v_+(-x, y) \quad \forall (x, y) \in \Omega_-.$$

With this choice we see that

$$K_{\mathcal{R}} = |\mu|,$$

and therefore for $|\mu| < 1$, (4) holds and Problem (6) has a unique solution. We further easily check that the corresponding mapping $\mathbb{T}$ is an isomorphism since $(\mathbb{T})^2 = \mathbb{T}$. Similarly on exchanging the roles of Ω_+ and Ω_-, (4) will also hold if $|\mu| > 1$. Now we take as the exact solution

$$u(x, y) = \mu x(x + 1)(x - 1)(y + 1)(y - 1) \ \forall (x, y) \in \Omega_+,$$
$$u(x, y) = x(x + 1)(x - 1)(y + 1)(y - 1) \quad \forall (x, y) \in \Omega_-,$$

f being fixed accordingly.

The finite element spaces V_h are built by using a global mesh refinement process from an initial Cartesian grid. More precisely the domain is decomposed into squares of size h and each square is divided into two triangles as shown in Fig. 2 for $h = 0.25$. For the well-posedness of the discrete problem, we can no longer use the symmetry transformation $\mathcal{R}$ because our triangulation is not symmetric with respect to the interface. Instead we use its discrete counterpart $\mathcal{R}_{e,h}$ defined as follows. First we define $\mathcal{R}_{e,h}(v_{h+})$ on the nodes of $\bar{\Omega}_-$:

$$\mathcal{R}_{e,h}(v_{h+})(x, y) = v_{h+}(-x, y) \quad \forall (x, y) \in \bar{\Omega}_- \cap \mathcal{N}_{\text{int}}.$$

Then $\mathcal{R}_{e,h}(v_{h+})$ is defined on each triangle of Ω_- by interpolation. Direct calculations show that

$$|\mathcal{R}_{e,h}(v_{h+})|_{1,\Omega_-} = |v_{h+}|_{1,\Omega_+}$$

and therefore

$$K_{\mathcal{R}_{e,h}} = |\mu|.$$

Consequently for $|\mu| < 1$, Problem (12) has a unique solution. As for the continuous problem, exchanging the role of Ω_+ and Ω_-, we get existence and uniqueness of Problem (12) if $|\mu| > 1$.

Let us recall that u_h is the finite element solution, and set $e_{L^2}(u_h) = \|u - u_h\|$ and $e_{H^1}(u_h) = \|u - u_h\|_1$ as the L^2 and H^1 errors. Moreover let us define $\eta(u_h) = \eta_R + \eta_J$ as the estimator and CV_{L^2} (resp. CV_{H^1}) as the experimental convergence rate of the error $e_{L^2}(u_h)$ (resp. $e_{H^1}(u_h)$) with respect to the mesh size defined by $\text{DoF}^{-1/2}$ computed from one line of the table to the following one (where DoF is the number of degrees of freedom).

Computations are performed with $\mu = -3$ using the meshes described above. First, it can be seen from Table 1 that the convergence rate of the H^1 error norm is equal to 1, as theoretically expected (see [9]). Furthermore the convergence rate of the L^2 error norm is 2, which is a consequence of the Aubin–Nitsche trick and regularity results for Problem (3). Finally, the reliability of the estimator is ensured since the ratio in the last column (the so-called effectivity index) converges towards a constant close to 6.5.

Table 1
The polynomial solution with $\mu = -3$ (uniform refinement).

k	DoF	$e_{L^2}(u_h)$	CV_{L^2}	$e_{H^1}(u_h)$	CV_{H^1}	$\frac{\eta(u_h)}{e_{H^1}(u_h)}$
1	289	2.37E−02		5.33E−01		6.70
2	1089	5.95E−03	2.08	2.67E−01	1.04	6.59
3	4225	1.49E−03	2.04	1.34E−01	1.02	6.53
4	16641	3.73E−04	2.02	6.68E−02	1.01	6.49
5	32761	1.89E−04	2.01	4.75E−02	1.01	6.48
6	90601	6.79E−05	2.01	2.85E−02	1.00	6.47
7	251001	2.45E−05	2.00	1.71E−02	1.00	6.47

5.2. A singular solution

This section is devoted to the treatment of a problem presenting a singular behavior. Here we analyze an example introduced in [6] and make precise some results from [6]. The domain $\Omega = (-1, 1)^2$ is decomposed into two subdomains $\Omega_+ = (0, 1) \times (0, 1)$ and $\Omega_- = \Omega \setminus \bar{\Omega}_+$; see Fig. 1. As before we take $a = 1$ on Ω_+ and $a = \mu < 0$ on Ω_-. According to Section 3 of [6], Problem (6) has a singularity S at $(0, 0)$ if $\mu < -3$ or if $\mu \in (-1/3, 0)$, given in polar coordinates by

$$S_+(r, \theta) = r^\lambda \left(c_1 \sin(\lambda\theta) + c_2 \sin\left(\lambda\left(\frac{\pi}{2} - \theta\right)\right)\right) \quad \text{for } 0 < \theta < \frac{\pi}{2},$$

$$S_-(r, \theta) = r^\lambda \left(d_1 \sin\left(\lambda\left(\theta - \frac{\pi}{2}\right)\right) + d_2 \sin(\lambda(2\pi - \theta))\right) \quad \text{for } \frac{\pi}{2} < \theta < 2\pi,$$

where $\lambda \in (0, 1)$ is given by

$$\lambda = \frac{2}{\pi} \arccos\left(\frac{1 - \mu}{2|1 + \mu|}\right),$$

and the constants c_1, c_2, d_1, d_2 are appropriately defined.
Now we show using the arguments of Section 2 that for $-\frac{1}{3} < \mu < 0$ and $\mu < -3$, the assumption (4) holds. As before we define

$$\mathcal{R}(v_+)(x, y) = \begin{cases} v_+(-x, y) & \forall (x, y) \in (-1, 0) \times (0, 1), \\ v_+(-x, -y) & \forall (x, y) \in (-1, 0) \times (-1, 0), \\ v_+(x, -y) & \forall (x, y) \in (0, 1) \times (-1, 0). \end{cases}$$

This extensiondefines an element of $H^1_-(\Omega_-)$ such that

$$\mathcal{R}(v_+) = v_+ \quad \text{on } \Sigma.$$

Moreover with this choice we have

$$\sup_{\substack{v \in H^1_+(\Omega_+) \\ v \neq 0}} \frac{|B_-(\mathcal{R}(v), \mathcal{R}(v))|}{B_+(v, v)} = 3|\mu|,$$

and therefore for

$$3|\mu| < 1,$$

we deduce that (4) holds.

To exchange the roles of Ω_+ and Ω_- we define the following extension from Ω_- to Ω_+: for $v_- \in H^1_-(\Omega_-)$, let

$$\mathcal{R}(v_-)(x, y) = v_-(-x, y) + v_-(x, -y) - v_-(-x, -y) \quad \forall (x, y) \in \Omega_+.$$

We readily check that it defines an element of $H^1_+(\Omega_+)$ such that

$$\mathcal{R}(v_-) = v_- \quad \text{on } \Sigma.$$

Moreover with this choice we have (using the estimate $(a + b + c)^2 \leq 3(a^2 + b^2 + c^2)$ valid for all real numbers a, b, c)

$$\sup_{v \in H^1_-(\Omega_-), v \neq 0} \frac{B_+(\mathcal{R}(v), \mathcal{R}(v))}{|B_-(v, v)|} \leq 3/|\mu|,$$

and therefore for

$$3/|\mu| < 1,$$

we deduce that (4) holds.

If the same uniform meshes as in the previous subsection are used, then by building discrete versions of the two continuous operators $\mathcal{R}$ (defined node by node and then by interpolation), one can again prove that Problem (12) has a

Table 2
The singular solution with $\mu = -5$, $\lambda \approx 0.46$ (uniform refinement).

k	DoF	$e_{L^2}(u_h)$	CV_{L^2}	$e_{H^1}(u_h)$	CV_{H^1}	$\frac{\eta(u_h)}{e_{H^1}(u_h)}$
1	289	1.60E−02		2.84E−01		2.57
2	1 089	8.66E−03	0.93	2.10E−01	0.45	1.94
3	4 225	4.63E−03	0.92	1.55E−01	0.45	1.46
4	16 641	2.47E−03	0.92	1.13E−01	0.45	1.09
5	32 761	1.80E−03	0.92	9.69E−02	0.46	0.95
6	90 601	1.13E−03	0.92	7.68E−02	0.46	0.76
7	251 001	7.08E−04	0.92	6.08E−02	0.46	0.61

Table 3
The singular solution with $\mu = -100$, $\lambda \approx 0.66$ (uniform refinement).

k	DoF	$e_{L^2}(u_h)$	CV_{L^2}	$e_{H^1}(u_h)$	CV_{H^1}	$\frac{\eta(u_h)}{e_{H^1}(u_h)}$
1	289	6.12E03		1.54E−01		18.77
2	1 089	2.59E−03	1.29	9.91E−02	0.66	15.04
3	4 225	1.08E−03	1.29	6.35E−02	0.66	12.06
4	16 641	4.46E−04	1.29	4.04E−02	0.66	9.66
5	32 761	2.88E−04	1.29	3.24E−02	0.66	8.65
6	90 601	1.49E−04	1.30	2.32E−02	0.66	7.33
7	251 001	7.66E−05	1.30	1.66E−02	0.66	6.21

Table 4
The singular solution with $\mu = -5$, $\lambda \approx 0.46$ (local refinement).

k	DoF	$e_{L^2}(u_h)$	CV_{L^2}	$e_{H^1}(u_h)$	CV_{H^1}	$\frac{\eta(u_h)}{e_{H^1}(u_h)}$
1	81	2.92E−02		3.79E−01		3.39
5	432	3.49E−03	2.54	1.40E−01	1.19	4.18
7	1 672	1.25E−03	1.52	8.04E−02	0.82	4.07
10	5 136	4.26E−04	1.92	4.90E−02	0.88	3.63
13	20 588	1.64E−04	1.37	3.14E−02	0.64	3.32
18	80 793	5.50E−05	1.60	1.80E−02	0.81	3.23
24	272 923	2.39E−05	1.37	1.17E−02	0.71	2.5

Table 5
The singular solution with $\mu = -100$, $\lambda \approx 0.66$ (local refinement).

k	DoF	$e_{L^2}(u_h)$	CV_{L^2}	$e_{H^1}(u_h)$	CV_{H^1}	$\frac{\eta(u_h)}{e_{H^1}(u_h)}$
1	81	1.41E−02		2.35E−01		23.59
4	363	1.93E−03	2.65	8.77E−02	1.31	34.86
7	1 566	4.94E−04	1.86	4.31E−02	0.97	33.10
11	5 981	1.23E−04	2.07	2.15E−02	1.04	33.17
16	25 452	2.98E−05	1.96	1.05E−02	0.99	34.65
24	106 827	7.36E−06	1.95	5.23E−03	0.97	33.89

unique solution for $-\frac{1}{3} < \mu < 0$ and $\mu < -3$. Obviously if adaptive meshes are used this approach is no longer valid, but since the determinant of the rigidity matrix is a polynomial in μ (its degree depends on the number of degrees of freedom), only a finite number of exceptional values of μ have to be excluded. Therefore for tests with adaptive meshes we have chosen the values $\mu = -5$ and $\mu = -100$ as for uniform meshes; since our solver does not encounter any resolution problem we can deduce that these values are convenient.

In summary, for our numerical tests, we have taken as the exact solution the singular function $u(x, y) = S(x, y)$ for $\mu = -5$ and $\mu = -100$, non-homogeneous Dirichlet boundary conditions on Γ being fixed accordingly; this solution is then approximated by using successively uniform and adaptive meshes.

First, with uniform meshes, we obtain the expected convergence rate of order λ (resp. 2λ) for the H^1 (resp. L^2) error norm; see Tables 2 and 3. There, for sufficiently fine meshes, we may notice that the effectivity index varies between 1 and 0.6 for $\mu = -5$ and between 9 and 6 for $\mu = -100$. From these results we can say that the effectivity index depends on μ; this is confirmed by the numerical results obtained by an adaptive algorithm (see below).

Secondly, an adaptive mesh refinement strategy is used, based on the estimator $\eta_T = \eta_{R,T} + \eta_{J,T}$, the marking procedure

$$\eta_T > 0.5 \max_{T'} \eta_{T'}$$

and a standard refinement procedure with a limitation on the minimal angle.

For $\mu = -5$ (resp. $\mu = -100$), Table 4 (resp. Table 5) displays the same quantitative results as before. There we see that the effectivity index is around 3 (resp. 34), which is quite satisfactory and comparable with results from [21,20]. As before and in these references we notice that it deteriorates as the contrast becomes larger. In these tables we also remark a convergence order of 0.76 (resp. 1) in the H^1-norm and mainly double that in the L^2-norm. This yields better orders of convergence as for uniform meshes as expected, the case $\mu = -5$ giving less accurate results due to the highly singular behavior of the solution (a similar phenomenon occurs in [21] for instance).

Acknowledgment

We are indebted to the anonymous referee for his/her valuable comments on the submitted manuscript, that allowed us to improve it significantly.

References

[1] N. Engheta, An idea for thin subwavelength cavity resonator using metamaterials with negative permittivity and permeability, IEEE Antennas Wirel. Propag. Lett. 1 (2002) 10–13.
[2] J. Ma, I. Wolff, Modeling the microwave properties of supraconductors, Trans. Microw. Theory Tech. 43 (1995) 1053–1059.
[3] D. Maystre, S. Enoch, Perfect lenses made with left-handed materials: Alice's mirror, J. Opt. Soc. Amer. A 21 (2004) 122–131.
[4] J.B. Pendry, Negative refraction makes a perfect lens, Phys. Rev. Lett. 85 (2000) 3966–3969.
[5] K. Ramdani, Lignes supraconductrices: analyse mathématique et numérique, Ph.D. Thesis, Université Pierre et Marie Curie, Paris, 1999.
[6] A.-S. Bonnet-BenDhia, M. Dauge, K. Ramdani, Analyse spectrale et singularités d'un problème de transmission non coercif, C. R. Acad. Sci. Paris Sér. I Math. 328 (8) (1999) 717–720.
[7] A.S. Bonnet-BenDhia, P. Ciarlet Jr., C.M. Zwölf, Two- and three-field formulations for wave transmission between media with opposite sign dielectric constants, J. Comput. Appl. Math. 204 (2) (2007) 408–417.
[8] A.-S. Bonnet-BenDhia, P. Ciarlet Jr., C.M. Zwölf, A new compactness result for electromagnetic waves. Application to the transmission problem between dielectrics and metamaterials, Math. Models Methods Appl. Sci. 18 (9) (2008) 1605–1631.
[9] A.S. Bonnet-BenDhia, P. Ciarlet Jr., C.M. Zwölf, Time harmonic wave diffraction problems in materials with sign-shifting coefficients, J. Comput. Appl. Math. 234 (6) (2010) 1912–1919.
[10] M. Ainsworth, J. Oden, A Posteriori Error Estimation in Finite Element Analysis, John Wiley and Sons, 2000.
[11] I. Babuška, T. Strouboulis, The Finite Element Methods and its Reliability, Clarendon Press, Oxford, 2001.
[12] P. Monk, Finite Element Methods for Maxwell's Equations, in: Numerical Mathematics and Scientific Computation, Oxford University Press, 2003.
[13] R. Verfürth, A Review of a Posteriori Error Estimation and Adaptive Mesh-Refinement Techniques, in: Wiley–Teubner Series Advances in Numerical Mathematics, Wiley–Teubner, Chichester, Stuttgart, 1996.
[14] P.G. Ciarlet, The Finite Element Method for Elliptic Problems, North-Holland, Amsterdam, 1978.
[15] P. Clément, Approximation by finite element functions using local regularization, RAIRO Anal. Numer. 2 (1975) 77–84.
[16] L.R. Scott, S. Zhang, Finite element interpolation of non-smooth functions satisfying boundary conditions, Math. Comp. 54 (1990) 483–493.
[17] M. Ainsworth, A posteriori error estimation for discontinuous Galerkin finite element approximation, SIAM J. Numer. Anal. 45 (4) (2007) 1777–1798 (electronic).
[18] S. Cochez-Dhondt, S. Nicaise, Equilibrated error estimators for discontinuous Galerkin methods, Numer. Methods Partial Differential Equations 24 (2008) 1236–1252.
[19] A. Ern, S. Nicaise, M. Vohralík, An accurate **H**(div) flux reconstruction for discontinuous Galerkin approximations of elliptic problems, C. R. Math. Acad. Sci. Paris 345 (12) (2007) 709–712.
[20] A. Ern, A.F. Stephansen, M. Vohralík, Guaranteed and robust discontinuous Galerkin a posteriori error estimates for convection–diffusion–reaction problems, J. Comput. Appl. Math. 234 (2010) 114–130.
[21] S. Cochez-Dhondt, S. Nicaise, A posteriori error estimators based on equilibrated fluxes, Comput. Methods Appl. Math. 10 (1) (2010) 49–68.